International Journal of Nanomedicine

Dovepress
open access to scientific and medical research

Open Access Full Text Article

ORIGINAL RESEARCH

Conjugation of glucosamine with Gd^{3+}-based nanoporous silica using a heterobifunctional ANB-NOS crosslinker for imaging of cancer cells

This article was published in the following Dove Press journal:
International Journal of Nanomedicine
23 September 2013
Number of times this article has been viewed

Bita Mehravi[1]
Mohsen Ahmadi[1]
Massoud Amanlou[2]
Ahmad Mostaar[1]
Mehdi Shafiee Ardestani[3]
Negar Ghalandarlaki[4]

[1]Biomedical Engineering and Medical Physics Department, Faculty of Medicine, Shahid Beheshti University of Medical Sciences, Tehran, Iran; [2]Department of Medicinal Chemistry, Faculty of Pharmacy and Drug Design and Development Research Center, Tehran University of Medical Sciences, Tehran, Iran, [3]Department of RadioPharmacy, Faculty of Pharmacy, Tehran University of Medical Sciences, [4]Department of Biological Science, School of Science, Science and Research Branch, Islamic Azad University, Tehran, Iran

Background: The aim of this study was to synthesize Gd^{3+}-based silica nanoparticles that conjugate easily with glucosamine and to investigate their use as a nanoprobe for detection of human fibrosarcoma cells.

Methods: Based on the structure of the 2-fluoro-2-deoxy-D-glucose molecule (^{18}FDG), a new compound consisting of D-glucose (1.1 nm) was conjugated with a Gd^{3+}-based mesoporous silica nanoparticle using an *N*-5-azido-2-nitrobenzoyloxy succinimide (ANB-NOS) crosslinker. The contrast agent obtained was characterized using a variety of methods, including Fourier transform infrared spectroscopy, nitrogen physisorption, thermogravimetric analysis, scanning and transmission electron microscopy, and inductively coupled plasma atomic emission spectrometry (ICP-AES). In vitro studies included cell toxicity, apoptosis, tumor necrosis factor-alpha, and hexokinase assays, and in vivo tests consisted of evaluation of blood glucose levels using the contrast compound and tumor imaging. The cellular uptake study was validated using ICP-AES. Magnetic resonance relaxivity of the contrast agent was determined using a 1.5 Tesla scanner.

Results: ANB-NOS was found to be the preferred linker for attaching glucosamine onto the surface of the mesoporous silica nanospheres. The r_1 relaxivity for the nanoparticles was 17.70 $mM^{-1}s^{-1}$ per Gd^{3+} ion, which is 4.4 times larger than that for Magnevist® (r_1 approximately 4 $mM^{-1}s^{-1}$ per Gd^{3+} ion). The compound showed suitable cellular uptake (75.6% ± 2.01%) without any appreciable cytotoxicity.

Conclusion: Our results suggest that covalently attaching glucosamine molecules to mesoporous silica nanoparticles enables effective targeted delivery of a contrast agent.

Keywords: gadolinium, glucosamine, mesoporous silica nanospheres, magnetic resonance imaging, *N*-5-azido-2-nitrobenzoyloxy succinimide, photoactivation

Introduction

Targeted delivery of a contrast agent mediated by functionalized nanoparticles is expected to improve imaging of cancer cells, enabling rapid diagnosis of the disease in its early stages.[1–3] In the past few years, mesoporous silica nanoparticles (MSNs) have emerged as an ideal nanoplatform in view of their biocompatibility and biodegradability. Numerous studies of the biocompatibility and toxicity of MSNs have been reported.[1–4] MSNs have a high surface area and large pore volumes for pay loading of magnetic centers and tunable particle size for efficient cellular uptake.[5–11] There has been interest in developing smart MSN nanocarriers with external and internal surfaces that can be selectively functionalized with multiple groups.[5,7–12] Contrast agents could also be covalently linked to these particles via cleavable bonds.[5,9,13,14] Further, abundant

Correspondence: Mohsen Ahmadi
Biomedical Engineering and Medical Physics Department, Faculty of Medicine, Shahid Beheshti University of Medical Sciences, Velenjak Street, Shahid Chamran Highway, Tehran, Iran.
Tel +98 21 2243 9941
Fax +98 21 2243 9941
Email dr.mohsen.ahmadi@gmail.com

© 2013 Mehravi et al, publisher and licensee Dove Medical Press Ltd. This is an Open Access article which permits unrestricted noncommercial use, provided the original work is properly cited.

silanol groups facilitate modification on their surfaces following synthesis. Most recently, surface-functionalized MSNs using cancer-specific agents have also been used for selectively targeting cancer cells.[15] Antibodies, peptides, aptamers,[16] carbohydrates,[17] and folic acid[18] are some of these agents. Glucose analogs are excellent agents for diagnosis of cancer, showing excessive cellular uptake of glucose due to overexpression of glucose transporters in cancer cells. Moreover, glucose consumption in these cells is very high because of their high rate of proliferation and angiogenesis.[19] Over the past decade, surface scientists have found that click reactions are powerful tools for binding functional groups onto a surface.[20,21] Clickable materials are species with click reaction capability, such as azide or alkyne groups. Click reactions are suitable for functionalization of silicon wafers as well as silicon rugate filters and the surface of mesoporous silica.[22] Some research work on clickable mesoporous silica nanoparticles has recently been reported.[23–26]

3-Aminopropyl trimethoxysilane (APTES) is an organosilane that is widely used for attaching targeting groups to the surfaces of MSNs. However, APTES does not contain a reactive functional group that could be used for covalent bonding with glucosamine. A stronger linkage could be achieved by attaching a heterobifunctional crosslinker, such as *N*-5-azido-2-nitrobenzoyloxy succinimide (ANB-NOS), to APTES for binding to glucosamine. ANB-NOS can covalently bind glucosamine through its aryl azide group following activation with ultraviolet light.[27]

This paper reports a simple novel method for synthesizing a nanoprobe containing MSNs loaded with Gd^{3+} and glucosamine (MSN-Gd^{3+}-DG) as a selective molecular imaging agent for human fibrosarcoma cells. Our in vitro and in vivo studies of conjugation of MSNs with glucosamine and Gd^{3+} loading indicate a novel nanoprobe with potential imaging effects in cancer cells.

Materials and methods

Materials

$GdCl_3 \cdot 6H_2O$ (99%), tetraethylorthosilicate (98%), methanol, anhydrous ethanol (99.5%), sodium hydroxide (NaOH), bromoacetic acid, cetyltrimethylammonium bromide (98%), APTES (99%), 3-(trimethoxysilylpropyl) diethylene triamine, anhydrous N,N dimethyl formamide (99.8%), toluene (99.8%), [4-(2-hydroxyethyl)-1-piperazineethanesulfonic acid] (HEPES), Tween 20, phosphate-buffered saline, and Infinity™ glucose reagent were purchased from Sigma-Aldrich (Seelze, Germany) and used without further purification. 3-(trimethoxysilylpropyl) diethylenetriamine was obtained from Gelest Inc (Morrisville, PA, USA). A dialysis bag with a 500–1000 Da cutoff was obtained from Spectrum Labs (Torrance, CA, USA). ANB-NOS was purchased from Pierce (Rockford, IL, USA). Other materials were sourced from Merck (Frankfurt, Germany). Fetal bovine serum and penicillin-streptomycin were also purchased from Sigma-Aldrich.

Human fibrosarcoma cells (HT1080) and murine mammary adenocarcinoma cells (derived from an M05 cell line) were purchased from the National Cell Bank of Pasteur Institute (Tehran, Iran). The HT1080 cells were cultured in Dulbecco's Modified Eagle's Medium supplemented with 5% fetal bovine serum (without heat inactivation) and 1% penicillin-streptomycin, and incubated at 37°C and 5% CO_2.

Instrumentation

The Gd^{3+} ions were quantified using inductively coupled plasma atomic emission spectrometry (ICP-AES, Optima 2300, Perkin-Elmer, Boston, MA, USA). The zeta potential of MSN-Gd^{3+}-DG dispersed in an aqueous solution (pH 7–8) was measured using a Zetasizer analyzer (Malvern Instruments Ltd, Worcestershire, UK). Transmission and scanning electron microscopic images were obtained on a Philips CM-120 (Eindhoven, The Netherlands) at 200 kV and a Hitachi 4160 (Tokyo, Japan), respectively. The textural properties of the MSN-Gd^{3+}-DG were obtained from nitrogen adsorption isotherms at 77 K using a Belsorp Mini device (Toyonaka City, Japan). Brunauer-Emmett-Teller surface areas were determined from the recorded adsorption data in the range of intermediate partial pressures $0.05 \leq P/P0 \leq 0.3$, and pore volume and pore size distribution were determined using the Barrett-Joyner-Halenda method. Thermogravimetric analysis was performed using a TGA-50 device (Shimadzu, Kyoto, Japan) equipped with a platinum pan at a heating rate of 3°C per minute under air.

Fourier transform infrared spectra were recorded using an Equinox 55 spectrophotometer (Bruker, Ettlingen, Germany). Magnetic resonance imaging (MRI) was performed on a 1.5 Tesla scanner (Siemens, Erlangen, Germany).

Flow cytometry was performed with a FACScan cytometer equipped with an Epics Altra HyPerSort 2 system (Beckman Coulter Inc, Fullerton, CA, USA) by counting 30,000 events, and the data were analyzed using Beckman Coulter software. Absorbance was measured at 450 nm using an ELX800 absorbance microplate reader (Bio-Tek Instruments Inc, Winooski, VT, USA). Blood glucose levels were measured using a glucometer (Bayer, Leverkusen, Germany).

Animals

BALB/C mice were sourced from the Laboratory Animal Center Institute of Cancer Research at Tehran University of Medical Sciences. The animal experiments were approved by the Imam Khomeini Cancer Research Center, Tehran, Iran. A total of 3×10^5 murine mammary adenocarcinoma cells (derived from an M05 cell line) were subcutaneously injected into the right flank of each mouse. Tumor growth was visible 4–5 weeks following injection.

Synthesis of MSN-Gd^{3+}-DG

Gd^{3+}-based MSNs

The MSNs used in this study were synthesized using the Stober method.[4] Briefly, 1.0 g of cetyltrimethylammonium bromide was dissolved in 500 mL of distilled water containing 3.5 mL of 2 M NaOH, and the solution was heated to 80°C. Next, 5.0 mL of tetraethylorthosilicate was added to the mixture. After stirring for a further three hours at 80°C, the MSNs were isolated by filtration and washed with distilled water and ethanol.

Amino-functionalized MSNs

First, 1.0 g of MSNs was dispersed in 100 mL of anhydrous ethanol with ultrasonic treatment for 10 minutes. Next, 1.0 mL of APTES was added dropwise to the solution over approximately 10 minutes and the reaction was stirred for 12 hours. The resulting solution was centrifuged at 6000 rpm for 20 minutes and redispersed in water to remove unreacted APTES.[28] The Kaiser test was performed to confirm that silanization was successful.[27]

Extraction of surfactant

The MSNs (1.5 g) were refluxed in 162 mL of methanol solution with 1.57 M hydrochloric acid for 12 hours to remove the surfactant (cetyltrimethylammonium bromide). The extracted MSN-NH_2 was washed three times with ethanol and stored as a dispersion in ethanol for future use.[29] Thermogravimetric analysis was used to characterize the amount of Gd^{3+}-diethylenetriamine tetraacetic acid (DTTA) embedded in the MSNs.

Synthesis of Si-DTTA

First, 0.4 g of 3-(trimethoxysilylpropyl) diethylene triamine and 1.0 g of bromoacetic acid were dissolved in 2.0 mL of distilled water and 4.0 mL of 2 M NaOH. The reaction solution was heated to 50°C. NaOH (6.0 mL, 2 M) was added dropwise over 20 minutes. After stirring for a further three hours at 50°C, the solvent was removed under reduced pressure to obtain a viscous yellowish oil. After washing with ethanol, a hygroscopic powder was obtained in high yield (>90%).[14]

Synthesis of Gd^{3+}-Si-DTTA

Si-DTTA (100.0 mg) was dissolved in 4.0 mL of distilled water by stirring at room temperature. Next, 300.0 µL of 50 M $GdCl_3$ was added dropwise to the solution. The pH of the solution was adjusted to about 9 by addition of 1 M NaOH. After stirring for three hours at room temperature, the resulting solution was then concentrated to 1.0 mL (Figure 1).[8,14]

Loading Gd^{3+}-Si-DTTA into MSN-NH_2

MSN-NH_2 (200.0 mg) was refluxed with 0.5 mL of the Gd^{3+}-Si-DTTA complex (0.1 M) in toluene for 48 hours.

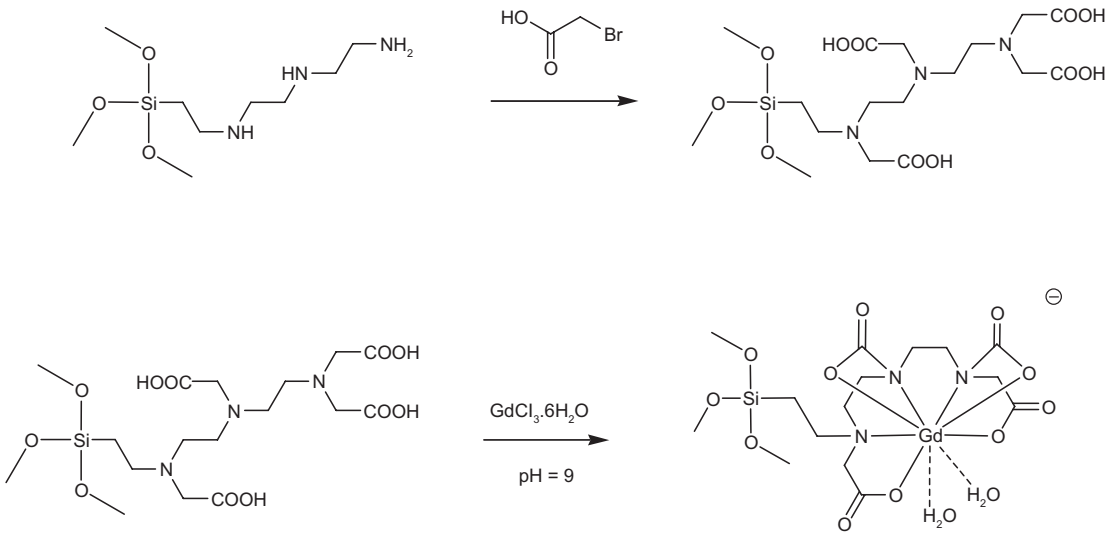

Figure 1 Schematic of DTTA and Gd^{3+}-DTTA synthesis.
Abbreviations: DTTA, diethylenetriamine tetraacetic acid; O, negatives charge.

The resulting MSN-NH_2-Gd^{3+}-Si-DTTA was centrifuged at 8000 rpm for 15 minutes, then washed with water and ethanol. The resulting nanoparticles were dialyzed against phosphate-buffered saline to ensure removal of any free complexes.[8,14]

Treatment of silanized surface with heterobifunctional ANB-NOS

ANB-NOS was dissolved in dimethyl formamide. Next, 500 mg of MSN-NH_2 and 50 mg of ANB-NOS were reacted in 20 mM HEPES at pH 8 and room temperature for two hours in the dark. The Kaiser test was performed to show successful reaction with ANB-NOS by confirming the absence of free amines.[27,29]

Conjugation of glucosamine

MSNs functionalized with 100.0 mg of ANB-NOS (MSN-ANB-NOS) was incubated at 37°C for 30 minutes with a saturated solution of glucosamine. Glucosamine was attached to the MSN surfaces by exposure to 302 nm light for five minutes at room temperature. Unbound glucosamine molecules were removed by washing three times with phosphate-buffered saline containing 0.05% Tween 20 (pH 7.5), with dialysis against phosphate-buffered saline to ensure removal of any free glucosamine molecules (Figure 2).[30,31]

Preparation for MRI in vitro

AnHT1080 cell line (1×10^5) was incubated with two different doses of MSN-Gd^{3+}-DG (0.2 µM and 0.4 µM) for one hour. The labeled cells were washed with phosphate-buffered saline, trypsinized, and then centrifuged at 1000 rpm for five minutes at 37°C. The cells were then resuspended in an equal volume of Dulbecco's Modified Eagle's Medium and 2% agarose gel at 37°C, and were immediately translocated into phantom tubes for the MRI procedure. Unlabelled cells were used as the control group.

Kaiser test for free amines

The Kaiser test was used to detect the presence of free amino groups on the surface of the MSNs. The samples were washed to remove unreacted APTES and ANB-NOS. The MSNs were then centrifuged at 6000 rpm for 10 minutes to remove the

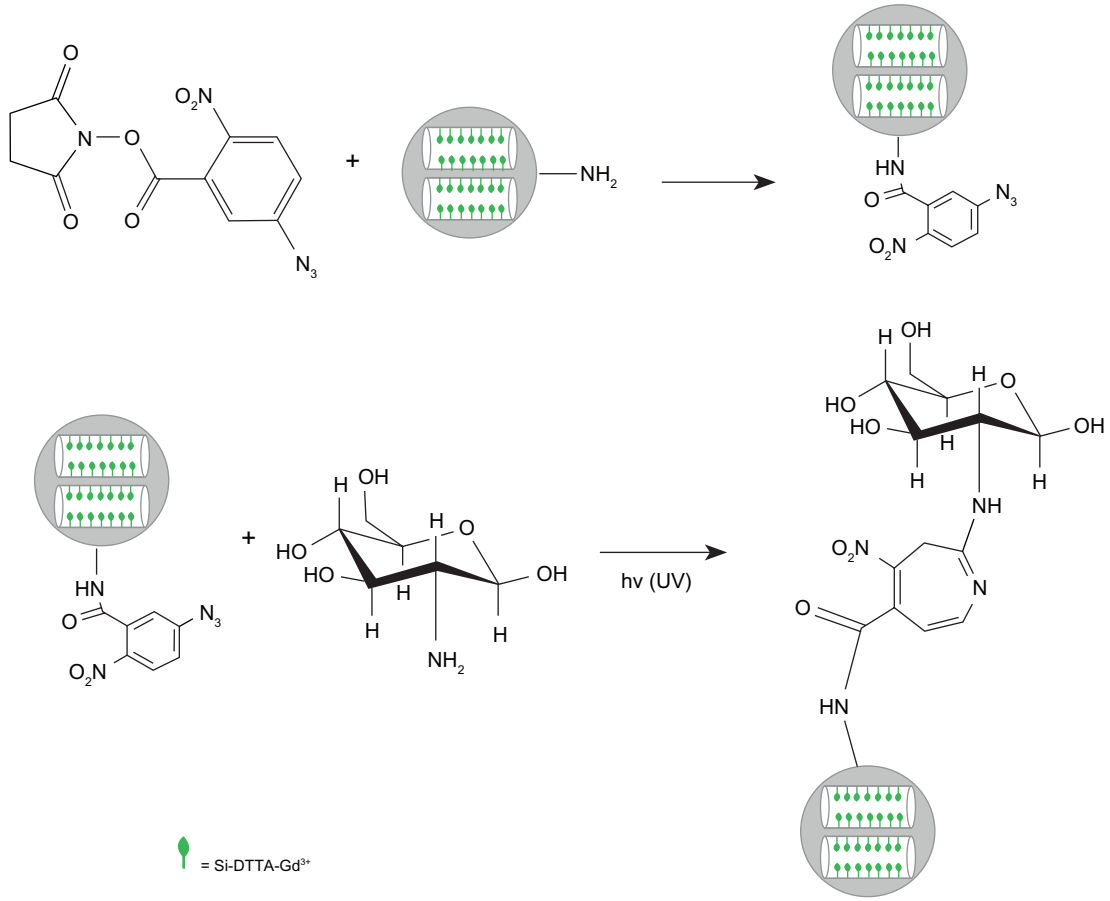

Figure 2 Schematic of synthesis of functionalized nanoparticles.
Abbreviations: hv (UV), ultra violet (302 nm); Si-DTTA, 3-Aminopropyl(trimethoxysilyl)diethylenetriamine tetraacetic acid; Si-DTTA-Gd, 3-Aminopropyl(trimethoxysilyl) diethylenetriamine tetraacetic acid (Si-DTTA) and its Gd complex.

supernatant. Solutions containing 50 mL of ninhydrin (0.5 g in 10 mL of ethanol), phenol (40 g in 10 mL of ethanol), and pyridine (1 mL of 0.001 M potassium cyanide in 49 mL of pyridine) were subsequently added to the MSNs. The MSN mixtures were then immersed in boiling water for two minutes. A blue color indicates the presence of free amine, whereas a yellow color indicates its absence.[27]

Cell viability (MTT) assay

The HT1080 cell line was cultured in 96-well plates (5×10^5 cells/well), with each well containing 200 µL of Dulbecco's Modified Eagle's Medium and 10% fetal bovine serum. After culture for 24 hours, the medium was removed and replaced with Dulbecco's Modified Eagle's Medium containing 1% fetal bovine serum in the absence or presence of two concentrations of MSN-Gd^{3+}-DG (100 nM, 200 nM) and incubated for 24 hours. Each concentration was tested in triplicate. MTT solution (20 µL of 5 mg/mL) was added to each well and incubated at 37°C for four hours in 5% CO_2; cellular reduction of MTT by mitochondrial dehydrogenase in viable cells forms a blue formazan product, which can be measured quantitatively by a microplate reader at a wavelength of 540 nm.[32]

TNF-α assay

The amount of tumor necrosis factor-alpha (TNF-α) secreted was analyzed using an enzyme-linked immunosorbent assay kit (U-CyTechR Biosciences, Utrecht, The Netherlands). MSN-Gd^{3+}-DG at 20, 40, 60, and 100 µg/mL was incubated with the HT1080 cell line for 24 hours. The cells were then pelleted and the supernatants collected for quantitative determination of TNF-α secretion according to a specific protocol at 570 nm, using a Bio-Tek absorbance microplate reader at 450 nm. The negative control contained only Dulbecco's Modified Eagle's Medium.[33,34]

Apoptosis assays

Apoptosis is considered a different mechanism of certain cell death. Apoptosis was determined using an Annexin V-propidium iodide staining kit according to the manufacturer's recommendations.[35]

Intracellular uptake study

To detect intracellular uptake of MSN-Gd^{3+}-DG, the cells were replated into six-well plates at a concentration of 2×10^5 cells per well and incubated at 37°C and 5% CO_2 for 24 hours. MSN-Gd^{3+}-DG (1 mL of 5.0 µg/mL) was added to the wells, each of which contained 1 mL of medium. The cells were incubated at 37°C with 5% CO_2 for two hours. The cells were washed twice with 500 µL of phosphate-buffered saline, and then centrifuged at 1000 rpm for four minutes and reconstituted in 100 µL of phosphate-buffered saline. Cellular uptake of Gd^{3+} ions was determined quantitatively by ICP-AES. From the concentration of Gd^{3+} ions and the total number of cells, the average amount of Gd^{3+} ions taken up by each cell was calculated. These measurements were performed in triplicate and the mean and standard deviation of the results were calculated.

Hexokinase assay

The hexokinase assay experiments were carried out according to a previous report.[36] Briefly, 1.0 mg of MSN-Gd^{3+}-DG and 1.0 mg of deoxyglucosamine were dissolved separately in 1.0 mL of water. Exactly 200 µL of each solution was diluted in 2.5 mL of water.[33] A 10 µL aliquot of each solution was mixed with 900 µL of Infinity glucose reagent and incubated at 37°C for three minutes. Changes in absorbance of Nicotinamide adenine dinucleotide phosphate (NADP) were measured using a Bio-Tek absorbance microplate reader at 450 nm.

Changes in blood glucose levels

Changes in blood glucose levels were investigated as described elsewhere.[33] Different doses of MSN-Gd^{3+}-DG (1, 5, 10 mg/kg) were injected intravenously into BALB/C mice (six per group). Changes in blood glucose levels were determined using a glucometer 30, 60, 90, 120, and 180 minutes after injection and were compared with levels in the control groups. The control groups were treated with insulin (a glucose-lowering agent, negative control) or glucosamine (a glucose-increasing agent, positive control), or received no treatment.

Statistical analysis

Multigroup comparisons of the means were carried out using one-way analysis of variance. Statistical significance for cell toxicity was set at $P < 0.05$, and for the TNF-α and apoptosis assays was set at $P < 0.05$ and $P < 0.01$, respectively. The results are expressed as the mean ± standard deviation (n = 3–5).

Measurements on MRI

Relaxation times for MSN-Gd^{3+}-DG were measured at different concentrations of 0.6, 0.3, 0.15, 0.075, and 0.0375 mM. Different spin echo and gradient echo protocols were used, with a 1.5 Tesla machine with a head coil. Multiple spin echo protocols were used for measurement of T_2. Standard spin

echo particulars were as follows: echoes 4; TE 16, 32, 48, 64 msec; TR 3000 msec; matrix 512*384; slice thickness 4 mm; field of view 25 cm; and NEX 3. A Flash protocol was used to compute the T_1 maps. Standard spin echo was as follows: echoes 1; TE 15 msec; TR 100, 200, 400, 600, 1000, and 2000 msec; matrix 512*384; slice thickness 4 mm; field of view 25 cm; NEX 3; and pixel bandwidth 130. For quantitative analysis of the data, the MRI images obtained were transferred to DICOM (Digital Imaging and Communication in Medicine) Works software version 1.3.5 (Digital Imaging and Communications in Medicine, Rosslyn, VA, USA).[33]

In vivo imaging of tumors

An MRI study was carried out in an animal model to evaluate the in vivo capability of the MSN-Gd^{3+}-DG to discriminate between cancerous and normal tissue. The tumor images obtained five minutes after a 5 μmol/kg injection showed that the amount of MSN-Gd^{3+}-DG internalized was large enough to have a significant effect on the intensity of the MRI signal.

Results

Qualitative characterization

The Kaiser test was used to detect the presence of priming amino groups on the surface of the MSNs.[23] APTES was used in this study to prepare priming amine groups for the particles by silanization. Once the reaction had taken place, the extracted MSN-NH_2 was washed to remove excess APTES. On addition of Kaiser solution, the particles turned blue immediately, indicating that APTES had been anchored. However, after addition of Kaiser solution to MSN-ANB-NOS, appearance of a yellow color indicated the absence of free amine.

Fourier transform infrared analysis

Fourier transform infrared spectroscopy was used to confirm the existence of functionalized MSNs in the region of 400–4000 cm^{-1}. The infrared spectrum of ANB-NOS showed absorption peaks at 1739 cm^{-1} and 1784 cm^{-1} attributable to C=O groups in the succinimide moiety, at 2120 cm^{-1} attributable to the N_3 group, and at 1527 cm^{-1} and 1348 cm^{-1} attributable to the NO_2 group.

When ANB-NOS was grafted onto the MSNs, the spectrum showed a new broad absorption band at 3200–3600 cm^{-1} corresponding to the silanol-OH bond and strong absorption of the siloxane (Si—O—Si) group at 1094 cm^{-1}. An N_3 absorption band was also observed at 2123 cm^{-1}, with an amide carbonyl (—NH—C=O) stretch mode at about 1637 cm^{-1}. These results indicate that ANB-NOS was incorporated into MSNs. When glucosamine was attached onto the MSN surface by exposure to light at 302 nm, the N_3 absorption disappeared and the OH groups on the MSN nanoparticles and glucosamine showed a broad band at 3000–3600 cm^{-1} (Figure 3).

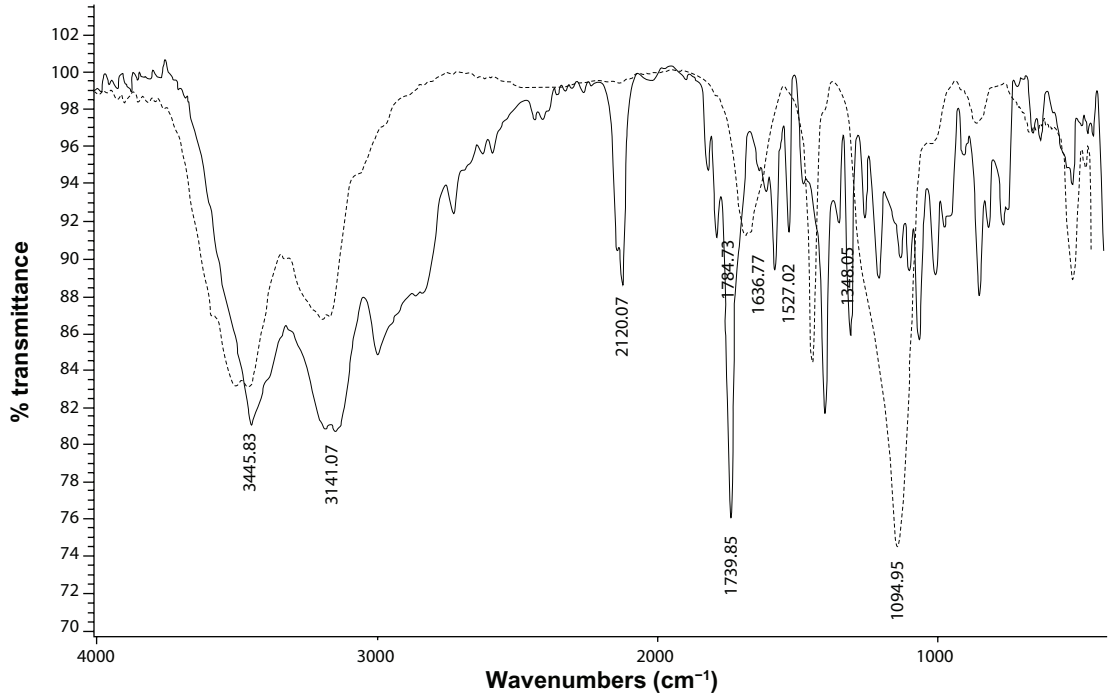

Figure 3 FTIR spectra of: (—) ANB-NOS-MSN; (----) glucosamine grafted on ANB-NOS-MSN: the N_3 absorption disappears when glucosamine was attached on the MSN surface.

Abbreviations: FTIR, fourier transform infrared spectroscopy; ANB-NOS-MSN, *N*-5-azido-2-nitrobenzoyloxy succinimide–mesoporous silica nanosphere; MSN, mesoporous silica nanospheres.

Adsorption and desorption of nitrogen

Measurements for adsorption and desorption of nitrogen gas indicated that the surfactant-extracted MSNs were highly porous, with a surface area of 970 m^2/g, an average pore diameter of 2.5 nm, and a total pore volume of 0.57 cm^3/g. In contrast, the MSN-Gd^{3+}-DG had a reduced surface area of 26.54 m^2/g, a mean pore diameter of 1.5 nm, and a total pore volume of 0.086 cm^3/g (Table 1).

Thermogravimetric analysis

Thermogravimetric analysis of the MSNs showed an initial weight loss of 13.7% from room temperature to 130°C for the adsorbed solvent species, and further weight loss of 46.99% in the temperature range of 160°C–290°C, indicating that the surfactant (cetyltrimethylammonium bromide) was removed, whereas the extracted MSNs showed a weight loss of 1.0% across a temperature range of 160°C–290°C. This result confirms that the surfactant was removed during extraction (Figure 4).

Electron microscopy

Scanning and transmission electron microscopy was used to evaluate MSN morphology and size. The images show that there was no change in MSN morphology after conjugation of glucose onto the surfaces of the MSNs, extraction of the surfactant, or upon grafting of the Gd^{3+}-DTTA-chelated molecule (Figures 5 and 6).

Zeta potential measurements

The zeta potentials for MSN, MSN-NH_2, and MSN-Gd^{3+}-DG are shown in Table 2, and indicate that the MSN-NH_2 aggregates in water because of the point of zero charge when pH is 7–8. In our experiments, although the MSN-NH_2 was washed three times after reaction, the ammonium hydroxide could not be completely removed. The solution appeared alkaline and had a low negative zeta potential of about −3 mV, indicating that the MSN-NH_2 aggregated rapidly, which agrees with the results reported by other researchers.[35,38,39]

Table 1 Summary of Barrett-Joiner-Halenda (BJH) surface areas and pore sizes

	Surface area (m^2/g) multipoint	Desorption isotherm	
		Total pore volume (cm^3/g)	Average pore diameter (nm)
MSN	60.27	0.085	1.8
Extracted MSN	970	0.57	2.5
MSN-Gd^{3+}-DG	26.54	0.086	1.5

Abbreviations: MSN, mesoporous silica nanospheres; extracted MSN, mesoporous silica nanospheres without surfactant; DG, D glucosamine; MSN-Gd^{3+}-DG, mesoporous silica nanospheres loaded with Gd^{3+} and conjugated with glucosamine.

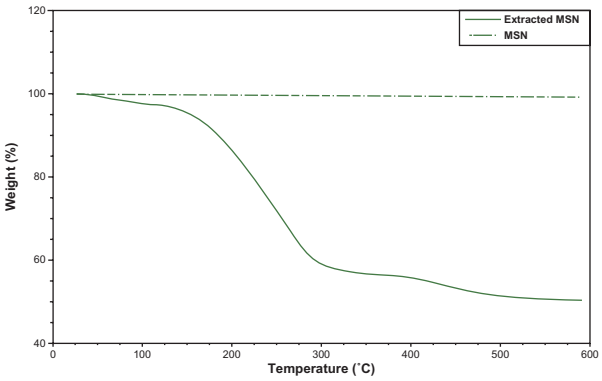

Figure 4 TGA curves of extracted MSN (—) and MSN (·—·). An initial weight loss of 13.7% from room temperature to 130°C for the adsorbed solvent species; Weight loss of 46.99% in the 160°C–290°C temperature range shows that the surfactant (CTABr) was removed.
Abbreviations: TGA, thermal gravimetric analysis; MSN, mesoporous silica nanospheres; extracted MSN, mesoporous silica nanospheres without surfactant; CTABr, cetyltrimethylammonium bromide.

Cell viability assay

MTT assays were performed using the HT1080 cell line to determine whether MSN-Gd^{3+}-DG has a cytotoxic effect. Figure 7 shows a comparison of the HT1080 cell line when incubated for 24 hours at different concentrations of MSN-Gd^{3+}-DG (100 µg/mL and 200 µg/mL). The MSN-Gd^{3+}-DG concentrations were similar to that of the control (0 µg/mL), indicating that cell viability was not affected at the concentration range tested.

TNF-α assay

Characterization of physiological effects is required for the continued development of MSN-Gd^{3+}-DG. The TNF-α level usually rises when cells are injured or inflamed. We found that treatment with MSN-Gd^{3+}-DG caused a significant increase in release of TNF-α up to a dose of 40 µg/mL ($P < 0.01$,

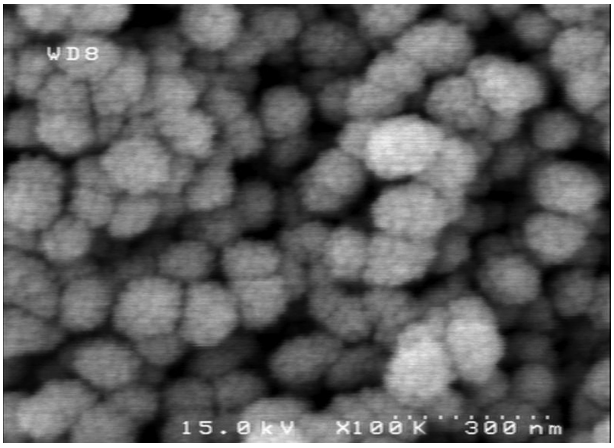

Figure 5 SEM images of MSN-Gd^{3+}-DG.
Abbreviations: SEM, scanning electron microscope; MSN-Gd^{3+}-DG, mesoporous silica nanospheres loaded with Gd^{3+} and conjugated with glucosamine.

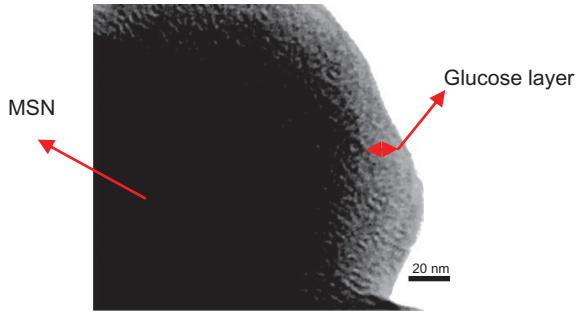

Figure 6 Transmission electron micrograph of an ultramicrotomed MSN-Gd^{3+}-DG. The layer of DG can be visualized by the rim of amphorous structure surrounding the MSN core with mesopores packed in a hexgonal symmetry.
Abbreviations: DG, D glucosamine; MSN, mesoporous silica nanospheres; MSN-Gd^{3+}-DG, mesoporous silica nanospheres loaded with Gd^{3+} and conjugated with glucosamine.

Figure 8). However, the increased dose of MSN-Gd^{3+}-DG did not have any toxic effects, such as causing cell death.

Apoptosis assay

Apoptosis is a mode of cell death that occurs under normal physiological conditions and the cell is an active participant in its own demise (ie, "cellular suicide"). Our findings demonstrate a statistically insignificant time-dependent increase in apoptotic cell responses to MSN-Gd^{3+}-DG at doses up to 40 µg/mL ($P < 0.05$); however, increasing the dose to over 60 µg/mL resulted in a significant increase in apoptotic activity. Further, it should be remembered that the results of the MTT assay indicated no toxic effects at any doses of MSN-Gd^{3+}-DG. Based on immunological assays, it can be hypothesized that if the exposure time is extended to over 24 hours, a significant increase in the rate of cell death is probable. The data analyzed are shown in detail in Figure 9.

Intracellular uptake study

The affinity of MSN-Gd^{3+}-DG for HT1080 cells was determined and compared with that obtained from the nonspecific precursor MSN-Gd^{3+}, as shown in Figure 10. The ICP-AES results show that cellular uptake of MSN-Gd^{3+}-DG was about 3.2 times more than that for the nanospheres alone. The data confirm the important role of glucose in MSN-Gd^{3+}-DG (Figure 10).

Hexokinase assay

Absorption at 340 nm for glucosamine and MSN-Gd^{3+}-DG (Table 3) was a sign of glucose phosphorylation due to the presence of the reduced form of nicotinamide adenine dinucleotide.[36,37]

Blood glucose levels

A statistically insignificant ($P < 0.05$) increase in blood glucose levels was observed after intravenous injection of MSN-Gd^{3+}-DG at the various doses.[36] Coadministration of MSN-Gd^{3+}-DG and insulin caused a marked decrease in blood glucose levels. This confirms the effectiveness of insulin on cell/tissue uptake of MSN-Gd^{3+}-DG (Figure 11).

In vitro MRI experiments

To evaluate whether the amount of MSN-Gd^{3+}-DG internalized was enough for visualization of cancerous cells with respect to healthy ones, an "in vitro" MRI experiment was performed. For this purpose, HT1080 cells were incubated for one hour in the presence of an equal amount (100 µM) of MSN-Gd^{3+}-DG. Figure 12 shows that cells labeled with MSN-Gd^{3+}-DG showed a more intense signal on the T_1-weighted spin echo image than the unlabeled cells. This demonstrates efficient uptake of the MSN-Gd^{3+}-DG for cell imaging.

Relaxivity

The MRI relaxation times for MSN-Gd^{3+}-DG were measured using a 1.5 Tesla MRI scanner (Figure 13). The nanoparticles showed large longitudinal (r_1) and transverse (r_2) relaxivities. The r_1 and r_2 values were 17.70 $mM^{-1}s^{-1}$ and 26.095 $mM^{-1}s^{-1}$, respectively and the r_2:r_1 ratio was 1.5 (Figure 14).

In vivo tumor imaging

The efficacy of MSN-Gd^{3+}-DG as an in vivo MRI contrast agent was evaluated. The tumor images obtained a few minutes after injection of MSN-Gd^{3+}-DG 5.0 µmol/kg via the tail vein indicate the usefulness of MSN-Gd^{3+}-DG as a potential MRI contrast agent (Figure 15).

Discussion

Gd^{3+}-based MSNs represent a nonselective contrast agent. Conjugation of glucosamine onto the surfaces of MSNs can be used to increase specific accumulation of these nanoparticles within the target cancerous tissue. Tumor cells consume more glucose than normal cells due to their higher rate of proliferation and overexpression of glucose transporters.[19]

Table 2 Characteristics of silica nanospheres (zeta potential)

Sample	Zeta potential (mV)	Average diameter	% intensity	Width (nm)	Polydispersity
MSN	−13.7	35.0	100	4.8	0.287
MSN-NH_2	+3.7	Aggregate			
MSN-Gd^{3+}-DG	−27.4	129	100	1.6	0.69

Abbreviations: MSN, mesoporous silica nanospheres; MSN-NH_2, amino-functionalized mesoporous silica nanospheres; MSN-Gd^{3+}-DG, mesoporous silica nanospheres loaded with Gd^{3+} and conjugated with glucosamine.

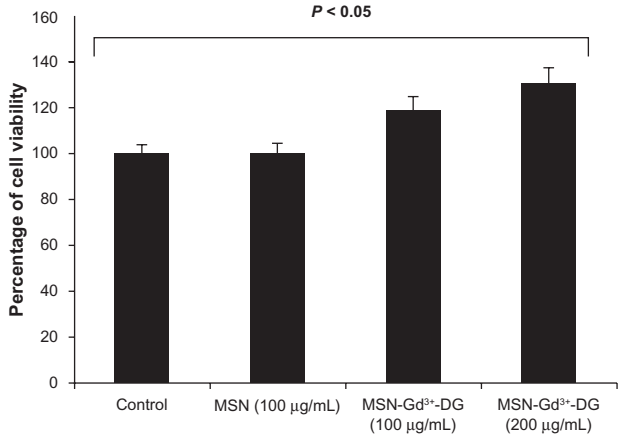

Figure 7 MTT results of 24 h of MSN-Gd^{3+}-DG exposure to HT1080; No significant toxic effect was observed ($P < 0.05$).
Abbreviations: MTT, MTT cell proliferation assay; HT1080, human fibrosarcoma cells; MSN, mesoporous silica nanospheres; MSN-Gd^{3+}-DG, mesoporous silica nanospheres loaded with Gd^{3+} and conjugated with glucosamine.

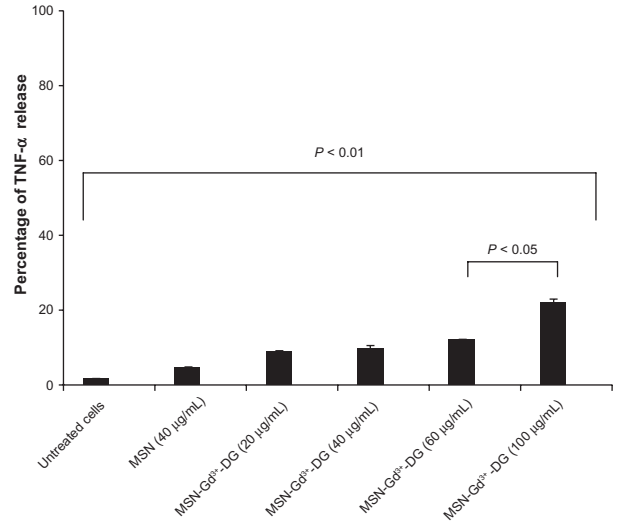

Figure 8 MSN-Gd^{3+}-DG treated HT1080 cells showed an insignificant release of TNF-α ($P < 0.05$, $P < 0.01$).
Abbreviations: TNF-α, tumor necrosis factor alpha; MSN-Gd^{3+}-DG, mesoporous silica nanospheres loaded with Gd^{3+} and conjugated with glucosamine; HT1080, human fibrosarcoma cells; MSN, mesoporous silica nanospheres.

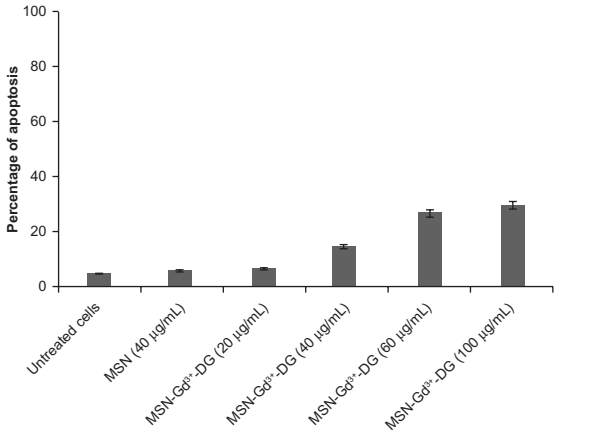

Figure 9 Apoptosis percentage of treated HT1080 cells with MSN-Gd^{3+}-DG ($P < 0.05$, $P < 0.01$).
Abbreviations: MSN-Gd^{3+}-DG, mesoporous silica nanospheres loaded with Gd^{3+} and conjugated with glucosamine; HT1080, human fibrosarcoma cells; MSN, mesoporous silica nanospheres.

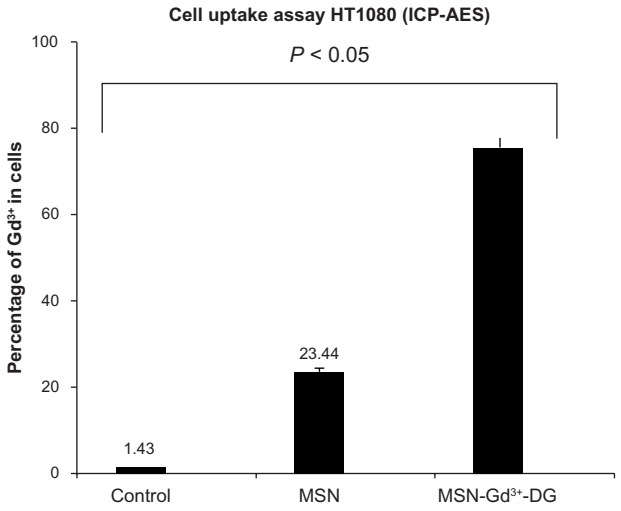

Figure 10 Cell uptake assay of MSN-Gd^{3+}-DG: Results indicated the glucose effect on intracellular uptake ($P < 0.05$).
Abbreviations: MSN-Gd^{3+}-DG, mesoporous silica nanospheres loaded with Gd^{3+} and conjugated with glucosamine; HT1080, human fibrosarcoma cells; ICP-AES, inductively coupled plasma atomic emission spectrometry; MSN, mesoporous silica nanospheres.

Amino-functionalized MSNs (MSN-NH_2) were prepared by silanization with 3-aminopropyltriethoxysilane. ANB-NOS is a heterobifunctional crosslinker containing an amine-reactive *N*-hydroxysuccinimide ester and a photoactivatable nitrophenyl azide. *N*-hydroxysuccinimide esters react with primary amino groups of MSN-NH_2 at pH 7–9 by forming a strong amide bond. When exposed to ultraviolet light, nitrophenyl azides form a nitrene group that can initiate additional reactions with double bonds and subsequent ring expansion to react with primary amines of glucosamine, which is a nucleophile. ANB-NOS is water-insoluble, so it was first dissolved in dimethyl formamide and then added to the aqueous reaction mixture. ANB-NOS is lipophilic and does not contain any charged groups. These properties are useful for intracellular conjugation.

MSN-NH_2 has many amine groups, which should be partially charged at pH 8.5. Since MSN-NH_2 does not have the ability to attach covalently to glucosamine directly the ANB-NOS is used for treating the surface of MSNs. ANB-NOS binds substantially more glucosamine molecules because the aryl azide group can link covalently with glucosamine. The crosslinking of ANB-NOS is initiated by

Table 3 Positive hexokinase enzyme response to glucosamine, and MSN-Gd^{3+}-DG

Glycosylated compounds at same concentration	Hexokinase activation after three minutes of incubation (340 nm)
Glucosamine	+
MSN-Gd^{3+}-DG	+

Abbreviation: MSN-Gd^{3+}-DG, mesoporous silica nanospheres loaded with Gd^{3+} and conjugated with glucosamine.

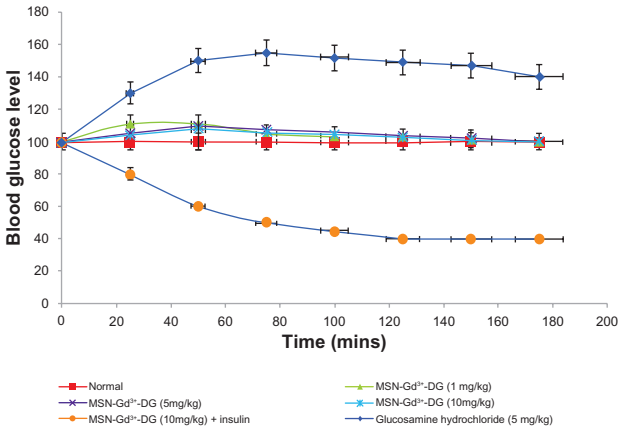

Figure 11 Effect of MSN-Gd^{3+}-DG on blood glucose level in rats. No significant changes were observed.
Abbreviation: MSN-Gd^{3+}-DG, mesoporous silica nanospheres loaded with Gd^{3+} and conjugated with glucosamine.

ultraviolet irradiation because ultraviolet light activates the aryl azide groups to nitrene. Via nitrene, some amino groups in glucosamine can be crosslinked to form amides. Nitrene is a very reactive functional group, so its participation in the cross-linking process takes less than 10^{-4} of a second,[37] which minimizes nonspecific binding.

MSNs have rigid and strained siloxyl groups on their surface, with glucosamine molecules bonded to the outside of a curved surface, which tend to have considerable freedom of movement.[38] Notwithstanding, ANB-NOS is relatively "bulky" (7.7 Å) and can probably saturate the curved surface. In this case, glucosamine fits onto the curved area, with multiple electrostatic interactions and without spatial restriction. Therefore, MSN-NH_2 can bind to glucosamine. The ANB-NOS-treated surface involves a covalent interaction, so glucosamine will remain attached. Accessibility of the surface to ANB-NOS is expected to be greater for a curved surface in comparison to a flatter surface.

MSN-Gd^{3+}-DG is transported inside the cell by specific glucose transporters and phosphorylated by hexokinase, but is not metabolized further to any significant extent. MSN-Gd^{3+}-DG-6-phosphate thereby accumulates in the cell, allowing distribution of MSN-Gd^{3+}-DG in the tissues to be imaged by MRI.

Figure 12 The significant positive signal enhancement in the T_1-weighted image was observed for the labeled cells compared with the unlabeled cells (HT1080 cell line [5×10^5]).
Abbreviation: HT1080, human fibrosarcoma cells.

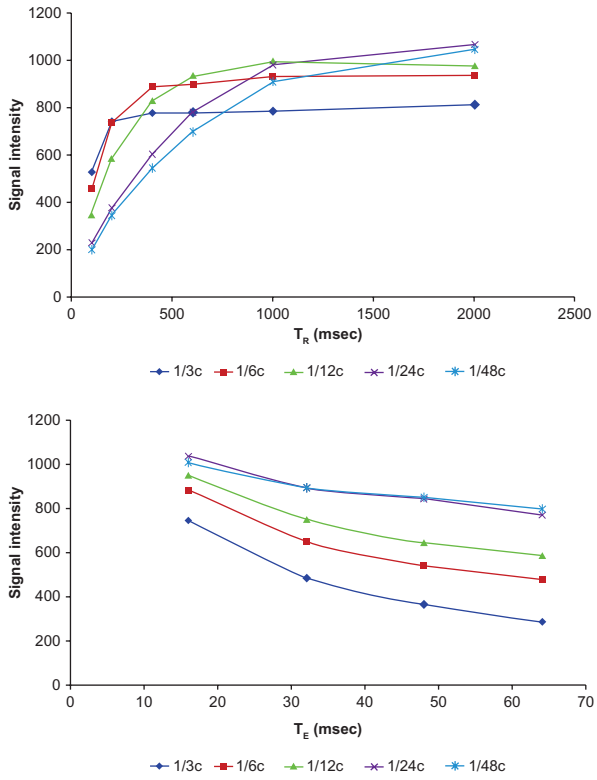

Figure 13 T_1 and T_2 data based on spin echo and gradient echo protocols.

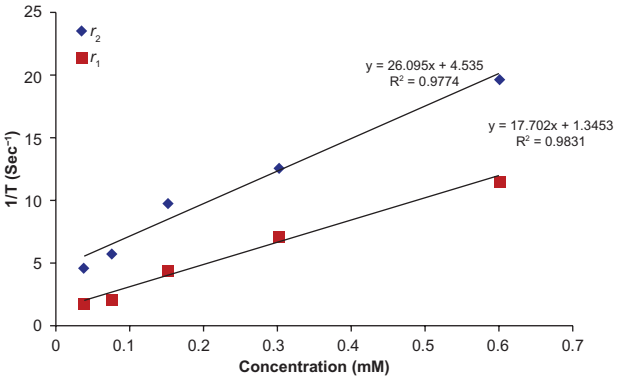

Figure 14 The r_1 and r_2 relaxivity curves of MSN-Gd^{3+}-DG.
Abbreviation: MSN-Gd^{3+}-DG, mesoporous silica nanospheres loaded with Gd^{3+} and conjugated with glucosamine.

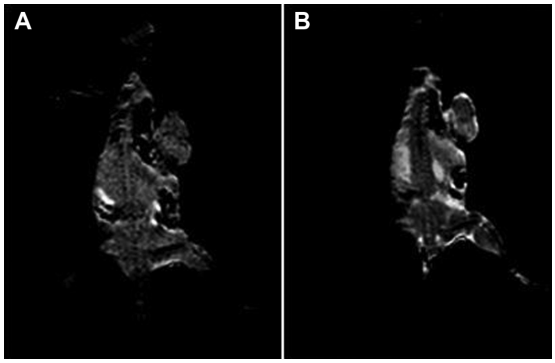

Figure 15 MR images (**A**) pre-injection and (**B**) 5 minutes post-injection (5 µmol/kg). A total of 3×10^5 Murine Mammary Adenocarcinoma Cells were subcutaneously injected into the right flank of a mouse. Tumor growth was visible 4–5 weeks post injection. This result shows the ability of MSN-Gd^{3+}-DG in enhancing the T_1-weighted images.
Abbreviations: MRI, magneic resonance imaging; MSN-Gd^{3+}-DG, mesoporous silica nanospheres loaded with Gd^{3+} and conjugated with glucosamine.

Glucosamine and MSN-Gd^{3+}-DG were tested for their ability to inhibit hexokinase competitively (Table 3). The behavior of MSN-Gd^{3+}-DG was similar to that of glucosamine for inhibition of hexokinase. Amanlou et al also conjugated D-glucose to diethylenetriamine penta-acetic acid, labeled it with Gd^{3+} (GDD), and examined the results in vitro and in vivo.[36] Their findings indicated that application of GDD to cancer cells also increased levels of TNF-α, but did not alter blood glucose levels. Interestingly, no toxicological findings were seen in normal human kidney cells.

Relaxivities were also measured, and the r_2:r_1 ratio was 1.3, indicating that MSN-NH_2-Gd^{3+} was a good T_1-weighted contrast agent. We attributed this enhanced MRI relaxivity to the accessibility of cellular water molecules at paramagnetic centers.

Detection of primary tumors is a critical issue in the treatment of cancer. We have designed a tumor-oriented MRI contrast agent based on glycosylated Gd^{3+}-based MSNs targeted to the glucose receptors overexpressed in tumor cells. Our results indicate that MSN-Gd^{3+}-DG can enhance T_1-weighted images. Taylor et al also prepared MSNs with grafted Gd^{3+} chelates (MSNs-Gd^{3+}) as T_1 contrast agents without any targeting group,[5] and demonstrated the efficacy of MSNs-Gd^{3+} as T_1 contrast agents both in vitro and in vivo. Their results suggested that MSNs- Gd^{3+} have good potential in the diagnosis of early disease.[5,11]

Comparison of the relaxivities of MSN-NH_2-Gd^{3+} and Magnevist® (Bayer HealthCare Pharmaceuticals, Inc, Montville, NJ, USA) (which has an r_1 value of 4.1 $mM^{-1}s^{-1}$ under the same conditions) shows that the former can be a better contrast agent. The same results were found comparing the relaxivity values of MSN-NH_2-Gd^{3+} with those of recently reported solid silica nanoparticles coated with multilayers of Gd^{3+}-DTTA.[8]

The effectiveness of MSN-NH_2-Gd^{3+} as an in vivo MRI contrast agent was evaluated using a 1.5 Tesla scanner. Upon injection of MSN-NH_2-Gd^{3+} 5 μmol/kg into the tail vein, significant T_1-weighted enhancement was clearly visible in the aortic and tumor tissue of a BALB/C mouse five minutes after injection (Figure 15), indicating the usefulness of MSN-NH_2-Gd^{3+} as an intravascular MRI contrast agent. This dose is much lower than what is typically required for currently used contrast agents (0.1–0.3 mmol/kg for Magnevist).[5,8,11] We attribute this to the large pore volume of MSNs for pay loading of magnetic centers (Gd^{3+}-Si-DTTA).

Conclusion

As expected, glucosamine did attach onto the MSN surface via the ANB-NOS crosslinker. The covalent bond formed between the silica surface and glucosamine is very resistant to disruption, and glucosamine has greater freedom of motion on the outside of a small sphere. Glucose-functionalized groups can be easily coupled to the surface of silica nanoparticles. Compared with existing methods, it is evident that covalent bonding of glucosamine to the MSN surface is an effective way of modifying MSNs. Immobilization of the Gd^{3+} ion inside the channels of MSNs enhances the transverse relaxation rate, leading to improved r_1 relaxivity. Using this design strategy, we expect that a new cellular imaging contrast enhancer can be available in the near future.

Acknowledgments

This work was supported by Shahid Beheshti Medical University and Tehran University of Medical Science. Authors thank Behroz Rafiei for valuable help with the 1.5 Tesla MRI system, and Maryam Shahzad Shirazi for valuable assistance with characterization analysis.

Disclosure

This research forms the major part of a PhD thesis by BM in nanomedicine. Otherwise, the authors report no conflicts of interest in this work.

References

1. Lu J, Liong M, Li Z, Zink JI, Tamanoi F. Biocompatibility, biodistribution, and drug-delivery efficiency of mesoporous silica nanoparticles for cancer therapy in animals. *Small*. 2010;6:1794–1805.
2. Guzman E, Liggieri L, Santini E, Ferrari M, Ravera F. Effect of hydrophilic and hydrophobic nanoparticles on the surface pressure response of DPPC monolayers. *J Phys Chem C*. 2011;115:21715–21722.
3. Guzman E, Liggieri L, Santini E, Ferrari M, Ravera F. Influence of silica nanoparticles on dilational rheology of DPPC-palmitic acid Langmuir monolayers. *Soft Matter*. 2012;8:3938–3948.
4. Yu T, Greish K, McGill LD, Ray A, Ghandehari H. Influence of geometry, porosity, and surface characteristics of silica nanoparticles on acute toxicity: their vasculature effect and tolerance threshold. *ACS Nano*. 2012;6:2289–2301.
5. Taylor KML, Kim JS, Rieter WJ, et al. Mesoporous silica nanospheres as highly efficient MRI contrast agents. *J Am Chem Soc*. 2008;130:2154–2155.
6. Lin W, Hyeon T, Lanza GM, Zhang M, Meade TJ. Magnetic nanoparticles for early detection of cancer by magnetic resonance imaging. *MRS Bull*. 2009;34:441–448.
7. Lin YS, Tsai CP, Huang HY, Kuo CT, HungY, Huang DM. Well-ordered mesoporous silica nanoparticles as cell markers. *Chem Mater*. 2005;17:4570–4573.
8. Lu J, Liong M, Sherman S, Xia T, Kovochich M. Mesoporous silica nanoparticles for cancer therapy: energy-dependent cellular uptake and delivery of paclitaxel to cancer cells. *Nanobiotechnology*. 2008;3:89–95.
9. Taylor-Pashow KML, Rocca JD, Lin W. Mesoporous silica nanoparticles with co-condensed gadolinium chelates for multimodal imaging. *Nanomaterials*. 2012;2:1–14.
10. Slowing II, Vivero-Escoto JL, Wu CW, Lin VSY. Mesoporous silica nanoparticles as controlled release drug delivery and gene transfection carriers. *Adv Drug Deliv Rev*. 2008;60:1278–1288.
11. Rieter W, Kim JS, Taylor KML, An H, Lin W, Tarrant TJ. Hybrid silica nanoparticles for multimodal imaging. *Angew Chem Int Ed*. 2007;46:3680–3682.

12. Kim JS, Rieter WJ, Taylor KML, An H, Lin W. Self-assembled hybrid nanoparticles for cancer-specific multimodal imaging. *J Am Chem Soc*. 2007;129:8962–8963.
13. Li LL, Yin Q, Cheng J, Lu Y. Polyvalent mesoporous silica nanoparticle-aptamer bioconjugates target breast cancer cells. *Adv Healthc Mater*. 2012;1:567–572.
14. De la Fuente JM, Penadés S. Glyconanoparticles: types, synthesis and applications in glycoscience, biomedicine and material science. *Biochim Biophys Acta*. 2006;1760:636–651.
15. Shen Z, Li Y, Kohama K, Oneill B, Bi J. Improved drug targeting of cancer cells by utilizing actively targetable folic acid-conjugated albumin nanospheres. *Pharm Res*. 2011;63:51–58.
16. Ganapathy V, Thangaraju M, Prasad PD. Nutrient transporters in cancer: relevance to Warburg hypothesis and beyond. *Pharm Ther*. 2009;121:29–40.
17. Schibli R, Dumas C, Petrig J. Synthesis and in vitro characterization of organometallic rhenium and technetium glucose complexes against glut 1 and hexokinase. *Bioconjug Chem*. 2005;16:105–112.
18. Khaniani Y, Badieia A, Ziarani GM. Application of clickable nanoporous silica surface for immobilization of ionic liquids. *J Mater Res*. 2012;27:931–938.
19. Haensch C, Hoeppener S, Schubert US. Chemical surface reactions by click chemistry: coumarin dye modification of 11-bromoundecyltrichlorosilane monolayers. *Nanotechnology*. 2008;19:035703.
20. Schlossbauer A, Schaffert D, Kecht J, Wagner E, Bein T. Click chemistry for high-density biofunctionalization of mesoporous silica. *J Am Chem Soc*. 2008;130:12558–12559.
21. Gallant ND, Lavery KA, Amis EJ, Becker ML. Universal gradient substrates for "click" biofunctionalization. *Adv Mater*. 2007;19:965–969.
22. Huang L, Dolai S, Raja K, Kruk M. "Click" grafting of high loading of polymers and monosaccharides on surface of ordered mesoporous silica. *Langmuir*. 2010;26:2688–2693.
23. Guan B, Ciampi S, Le Saux G, Gaus K, Reece PJ, Gooding JJ. Different functionalization of the internal and external surfaces in mesoporous materials for biosensing applications using "click" chemistry. *Langmuir*. 2011;27:328–334.
24. Wong C, Burgess JP. Modifying the surface chemistry of silica nanoshells for immunoassays. *J Young Invest*. 2003;6(1):1–14.
25. Boiteau R, Meade T. Gadolinium-labeled nanoparticles for magnetic resonance imaging. *Nanoscape*. 2008;5:33–39.
26. Radu DR, Lai CY, Wiench JW, Pruski M, Lin VS. Gatekeeping layer effect: a poly(lactic acid)-coated mesoporous silica nanospheres-based fluorescence probe for detection of amino-containing neurotransmitters. *J Am Chem Soc*. 2004;126:1640–1641.
27. McDonald AR, Dijkstra HP, Suijkerbuijk BMJM, van Klink GPM, van Koten G. "Click" immobilization of organometallic pincer catalysts for C-C coupling reactions. *Organometallics*. 2009;28:4689–4699.
28. Adams CA, Kar SR, Hopper JE, Fried MG. Self-association of the amino-terminal domain of the yeast TATA-binding protein. *J Biol Chem*. 2004;279:1376–1382.
29. Zhang C, Li Y, Shi X, Kim SK. Inhibition of the expression on MMP-2, 9 and morphological changes via human fibrosarcoma cell line by 6,6′-bieckol from marine alga Ecklonia cava. *BMB Rep*. 2009:62–68.
30. Amanlou M, Siadat SD, Ebrahimi SE, et al. Gd^{3+}-DTTA-DG: novel nanosized dual anticancer and molecular imaging agent. *Int J Nanomedicine*. 2011;6:747–763.
31. Mosmann T. Rapid colorimetric assay for cellular growth and survival: application for proliferation and cytotoxicity assay. *J Immunol Methods*. 1983;65:55–63.
32. Mirzaei M, Mohagheghi M, Shahbazi-Gahrouei D, Khatami A. Novel nanosized Gd^{3+}-ALGD-G2-C595: in vivo dual selective MUC-1 positive tumor molecular MR imaging and therapeutic agent. *J Nanomed Nanotechnol*. 2012;3:147–152.
33. Puech PA, Boussel L, Belfkih S, Lemaitre L, Douek P, Beuscart R. DicomWorks: software for reviewing DICOM studies and promoting low-cost teleradiology. *J Digit Imaging*. 2007;20:122–130.
34. Lewis RV, Roberts MF, Dennis EA, Allison WS. Photoactivated heterobifunctional cross-linking reagents which demonstrate the aggregation state of phospholipase. *Biochemistry*. 1977;16:5650–5654.
35. Iler RK. *The Chemistry of Silica*. New York, NY: John Wiley & Sons; 1979.
36. Amanlou M, Siadat SD, Ebrahimi SE, et al. Gd^{3+}-DTPA-DG: novel nanosized dual anticancer and molecular imaging agent. *Int J Nanomed*. 2011;6:747–763.
37. Schibli R, Dumas C, Petrig J. Synthesis and in vitro characterization of organometallic rhenium and technetium glucose complexes against GLUT 1 and hexokinase. *Bioconjug Chem*. 2005;16:105–112.
38. An Y, Chen M, Xue Q, Liu W. Preparation and self-assembly of carboxylic acid functionalized silica. *J Colloid Interface Sci*. 2007;31:507–513.
39. Slowing I, Trewyn BG, Lin VS. Effect of surface functionalization of MCM-41-type mesoporous silica nanoparticles on the endocytosis by human cancer cells. *J Am Chem Soc*. 2006;128:14792–14793.

International Journal of Nanomedicine Dovepress

Publish your work in this journal

The International Journal of Nanomedicine is an international, peer-reviewed journal focusing on the application of nanotechnology in diagnostics, therapeutics, and drug delivery systems throughout the biomedical field. This journal is indexed on PubMed Central, MedLine, CAS, SciSearch®, Current Contents®/Clinical Medicine, Journal Citation Reports/Science Edition, EMBase, Scopus and the Elsevier Bibliographic databases. The manuscript management system is completely online and includes a very quick and fair peer-review system, which is all easy to use. Visit http://www.dovepress.com/testimonials.php to read real quotes from published authors.

Submit your manuscript here: http://www.dovepress.com/international-journal-of-nanomedicine-journal